



HAL
open science

Geochemical variations in early Islamic glass finds from Bukhara (Uzbekistan)

Nadine Schibille, Catherine Klesner, Daniel R Neuville, Sören Stark, Asan I Torgoev, Sirojiddin J Mirzaakhmedov

► **To cite this version:**

Nadine Schibille, Catherine Klesner, Daniel R Neuville, Sören Stark, Asan I Torgoev, et al.. Geochemical variations in early Islamic glass finds from Bukhara (Uzbekistan). *Chemie der Erde / Geochemistry*, 2024, 84 (1), pp.126078. 10.1016/j.chemer.2024.126078 . hal-04551641

HAL Id: hal-04551641

<https://hal.science/hal-04551641>

Submitted on 18 Apr 2024

HAL is a multi-disciplinary open access archive for the deposit and dissemination of scientific research documents, whether they are published or not. The documents may come from teaching and research institutions in France or abroad, or from public or private research centers.

L'archive ouverte pluridisciplinaire **HAL**, est destinée au dépôt et à la diffusion de documents scientifiques de niveau recherche, publiés ou non, émanant des établissements d'enseignement et de recherche français ou étrangers, des laboratoires publics ou privés.



Contents lists available at ScienceDirect

Geochemistry

journal homepage: www.elsevier.com/locate/chemer

Geochemical variations in early Islamic glass finds from Bukhara (Uzbekistan)

Nadine Schibille^{a,*}, Catherine Klesner^{b,c}, Daniel R. Neuville^d, Sören Stark^c, Asan I. Torgoev^e, Sirojiddin J. Mirzaakhmedov^f

^a Institut de recherche sur les archéomatériaux, Centre Ernest-Babelon (IRAMAT-CEB), UMR7065, CNRS/Université d'Orléans, 45071 Orléans, France

^b McDonald Institute for Archaeological Research, University of Cambridge, Downing Street, Cambridge CB2 3ER, UK

^c Institute for the Study of the Ancient World, New York University, New York City, 10028, NY, USA

^d Université de Paris, Institut de physique du globe de Paris (IPGP), CNRS-UMR 7154, Paris 75005, France

^e State Hermitage, Saint Petersburg 190000, Russia

^f Samarkand Archaeological Institute, Cultural Heritage Agency of the Republic of Uzbekistan, Samarkand 140061, Uzbekistan

ARTICLE INFO

Handling Editor: Vincenza Guarino

Keywords:

LA-ICP-MS

Raman

Samarra

Silk roads

Central Asia

Plant ash glass

High alumina glass

Silica networks

Network modifiers

ABSTRACT

Glass manufacturing processes and recipes changed fundamentally after the 8th century CE. The earlier centralised production system diversified, primary production sites multiplied, and the scale of individual productions contracted. Mineral soda was no longer used and instead replaced by plant ash as the main fluxing agent, affecting the chemical composition and properties of the glass. In this work, LA-ICP-MS and Raman spectroscopy were used to investigate the compositional and structural characteristics of 68 glass fragments recovered during recent excavations at Bukhara in Uzbekistan, dating to the 9th to early 11th centuries CE. This is the most extensive systematically collected and studied glass assemblage from Central Asia to date. The glass can be attributed to different origins, confirming on the one hand the diversification of glass production during the early Islamic period and, on the other hand, regional variations in the chemical compositions and network structure of soda-rich plant ash glasses. As clear archaeological evidence for early Islamic glass production sites in Central Asia is rare, regional production groups are distinguished primarily on relative concentrations of Mg, K, P, Cl, Li and Cs in relation to the plant ash component, while variabilities in Al, Ti, Cr, Y, Zr, Th and REEs and their ratios indicate different silica sources. Raman spectra suggest variations in network connectivity and Q^n speciation that confirm compositional groupings and suggest structural differences between regional productions of plant ash glass. The results demonstrate a clear dominance of local or regional glass groups, while revealing the importation of Mesopotamian glass, notably a high-end colourless glass type from the region around Samarra in Iraq. The new analytical data allow further separation and characterisation of novel early Islamic plant-ash glass types and their production areas.

1. Introduction

Towards the end of the first millennium CE, glass making and circulation underwent significant changes. By the 10th century CE, primary production of glass, based on the use of soda-rich plant ash as the main alkali source, appears to have been established throughout the Islamic world, from Spain in the west to Central Asia in the east (for a review see (Schibille, 2022) and references therein). The classification of distinct glass groups and the identification of production areas have been hampered by the complex nature of plant ash glass, which is made from two highly variable raw materials, sand and plant ash, and their

seemingly arbitrary combination (e.g. Ganio et al., 2013; Mirti et al., 2009; Mirti et al., 2008; Schibille et al., 2022; Swan et al., 2017). The increasing number of elemental and isotopic data are gradually making it possible to isolate plant ash glass types and, consequently, primary production zones (Henderson et al., 2016; Henderson et al., 2020; Phelps, 2018; Schibille, 2022). Key questions are how to convert primary chemical data into meaningful glass groups and what level of internal variability can be tolerated. A detailed and comprehensive evaluation of analytical and structural data of well-contextualised glass assemblages is required to obtain viable groupings. Changes in the archeo-vitreous record over time and space can in turn provide insights

* Corresponding author.

E-mail address: nadine.schibille@cnrs.fr (N. Schibille).

<https://doi.org/10.1016/j.chemer.2024.126078>

Received 13 September 2023; Received in revised form 30 November 2023; Accepted 3 January 2024

Available online 7 January 2024

0009-2819/© 2024 The Authors. Published by Elsevier GmbH. This is an open access article under the CC BY-NC-ND license (<http://creativecommons.org/licenses/by-nc-nd/4.0/>).

into trade networks and the ancient economy, as well as the transfer of technologies and movement of goods and people.

This study presents the results of laser ablation inductively coupled plasma mass spectrometry (LA-ICP-MS) and Raman analyses of glass finds from Bukhara, one of the most important early Islamic metropolises within the ancient exchange networks of Central Asia in Uzbekistan (Fig. 1; Stark, 2018; Stark et al., 2016; Stark et al., 2022). The samples were recovered during ongoing rescue excavations by the Uzbek-American Expedition to Bukhara (UzAmEB), a collaboration between the Samarkand Institute of Archaeology under the Agency of Cultural Heritage of the Republic of Uzbekistan and the Institute for the Study of the Ancient World at New York University (Mirzaakhmedov et al., 2023). Within the framework of the UzAmEB project, systematic excavations were carried out in targeted areas across a sector of ca. 0.75 ha in the inner city, immediately to the north of the city's Congregational Mosque and east of the citadel, along the main east–west thoroughfare of the early medieval city (present-day Nurobod Street, Fig. 2). The project, which began in 2020, revealed a wide array of new archaeological data, transforming our understanding of the city's long and multi-layered history, such as previously unknown monumental fortifications dating to the centuries around the turn of our era, the first ever excavated domestic architecture in the city, dating to the 4th–5th centuries CE, and the 5th–10th-centuries CE western wall of shahristan (inner city) just to the north of the former Banu Asad gate mentioned in Narshakhi's 10th-century CE *Tarikh-i Bukhara* (History of Bukhara; Narshakhi, 1954). In particular, the excavations produced an incredibly large corpus of glass and glazed ceramics dated to the Samanid and early Qarakhanid periods (10th–11th centuries CE).

This rich collection of glass and glazed ceramic fragments provided the perfect opportunity to explore the archaeo-vitreous record of Bukhara from a controlled and reliably dated context. The aim of this study is to understand the evolution and spread of early Islamic glass production and circulation along the Silk Road network and to start mapping glass compositions and structural variations as a proxy of technological developments and transfer. These new data enable us to frame Central Asian glassmaking within the wider setting of Islamic glass production. A comparison with data from other Central Asian sites

such as Merv and Samarkand can identify the probable origins based on the frequency distributions of a particular type of glass and the degree of recycling. Our results lend support to an increasingly diversified glass production model in the early Islamic period and highlight the central role of glass in the economy of early Islamic Bukhara.

While compositional data obtained by LA-ICP-MS have been extensively used to classify archaeological glass, the use of Raman spectroscopy to characterise the network structure of silicate glasses is relatively new. Raman can yield additional insights into the structural organisation of the silica tetrahedra and their three-dimensional atomic arrangement. The distinct vibrations of T-O-T tetrahedra (T = network former Si) are strongly related to the chemical composition of the glass and more specifically to the network forming and network modifying cations. The T-O bonds are typically stronger than the M-O bonds (M = network modifiers) inasmuch as the latter interrupt bridging oxygens (BO) and determine the distribution of non-bridging oxygens (NBO). Raman-based models have been used in earth sciences (e.g. Giordano et al., 2019) to predict physical properties such as the viscosity of glass melts, which is critical for understanding glassmaking and glass working processes.

2. Materials and methods

2.1. Samples & sampling strategy

The vast majority of glass finds from the UzAMEB excavations come from the >50 refuse-filled garbage wells (*badrabs*) and cesspits (*tashnaus*) registered in the excavated areas since 2020 (Fig. 2). Such *badrabs* and *tashnaus* are characteristic of Central Asian cities of the 10th to early 13th centuries CE (Anarbaev, 1981; Mir-Makhamad et al., 2023). In Bukhara, *badrabs* are typically round, simple pits (diameters = 70–130 cm), which were often dug >7 m deep, i.e. beyond the depth of the present-day water table; *tashnaus* were of a similar depth but with a slightly smaller diameter, and they were either lined with fired bricks or large storage vessels with the bases removed. Both the *badrabs* and *tashnaus* were filled with sediments containing botanical and entomological remains, as well as large quantities of glass, ceramics and metals,

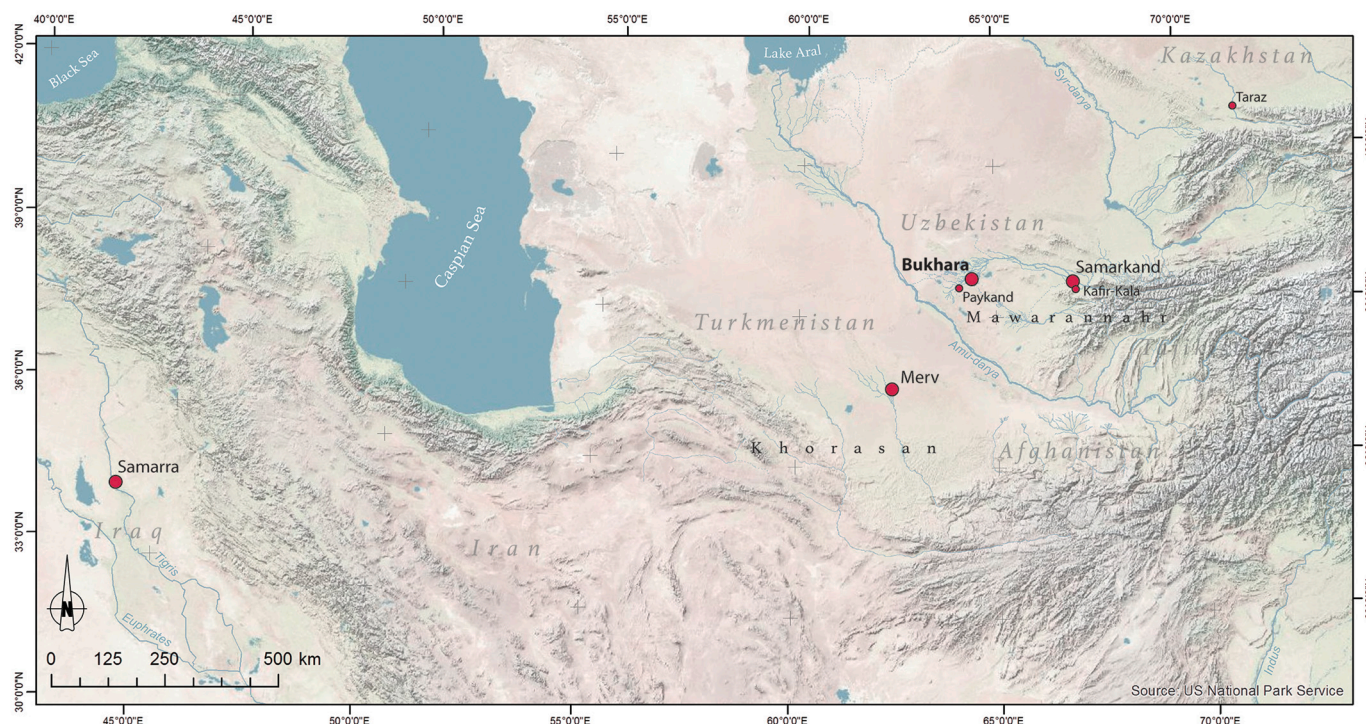


Fig. 1. Map showing the early Islamic world between Samarra in the west and Taraz in the east. Sites mentioned in the text are indicated.



Fig. 2. Excavations in the city centre of Bukhara. Satellite image of the excavation area is indicated in greenish yellow, the inserts are two drone aerial photographs showing the area prior to the excavations (left) and at the end of the 2022 season (right). The situational view of Badrab SU 28 and Tashnau SU 78 from the 2022 season is shown below. (For interpretation of the references to colour in this figure legend, the reader is referred to the web version of this article.)

and some animal bones (Mir-Makhamad et al., 2023). Thanks to abundant diagnostic ceramic and coin finds the *badrabs* and *tashnaus* in the area can be reliably dated to the 10th century CE, with the exception of two contexts (242, 163) where the chronology extends into the 9th and 11th century, respectively (Supplementary Table S1). The ubiquitous

presence of these waste pits just outside the western city wall to the north of the main western city gate (the Banu Asad gate) strongly suggests the existence of a small extramural bazaar in this area during the Samanid and early Qarakhanid periods, where travellers to and from the city gathered.

The total archaeological assemblage of glass artefacts retrieved from the UzAmEB excavations between 2020 and 2023 amounts to several thousand pieces and include a wide range of glass types. Two *badrabs* (SU18 and SU28) and one *tashnau* (SU 73) in Trench 2 (Fig. 2) returned a particularly large number of glass finds, possibly indicating a nearby glass workshop and/or merchant. A total of 68 glass shards from the 2021 and 2022 excavation seasons were deemed representative of the entire collection and thus selected for compositional analysis. Pieces were chosen to include the range of glass colours, vessel forms, and technological aspects (free blown, moulded, wheel cut, applied and pinched decorations) and samples were selected in an attempt to not duplicate any individual vessels (e.g. only one fragment of window glass was selected from each stratigraphic unit). The glass types (Supplementary Table S2) were characterised following Kröger (1995), and include samples of free-blown ($n = 51$) and mould-blown vessels ($n = 9$) with a range of decorations including applied ($n = 3$), incised ($n = 1$),

pinched ($n = 8$), and wheel-cut decorations ($n = 7$; Fig. 3). The finds also comprise fragments of window glass ($n = 6$), which have a folded outer rim and diameters of up to 47 cm. The Bukhara assemblage is noted for a large number of alembic vessels ($n = 3$), which have a cylindrical or globular body with an open neck and a long spout. It is thought that they were used for distillation or medical purposes (Kröger, 1995). Most of the glass present in the assemblage is transparent and colourless (i.e. not intentionally coloured). However, there are samples of blue ($n = 3$), turquoise ($n = 2$), and purple ($n = 1$) coloured glass, and blue decorations were applied to one example (BKH21-211-6).

An additional three samples of raw glass chunks were included in the analysis. Two of these fragments were recovered from excavations at the site of Paykand (Abdurazakov, 1998), a possible early Islamic glass workshop located ca. 40 km to the southeast just outside the Bukhara Oasis. An additional glass ingot was sampled from Taraz about 860 km north-east of Bukhara. Both of these are smaller cities that were

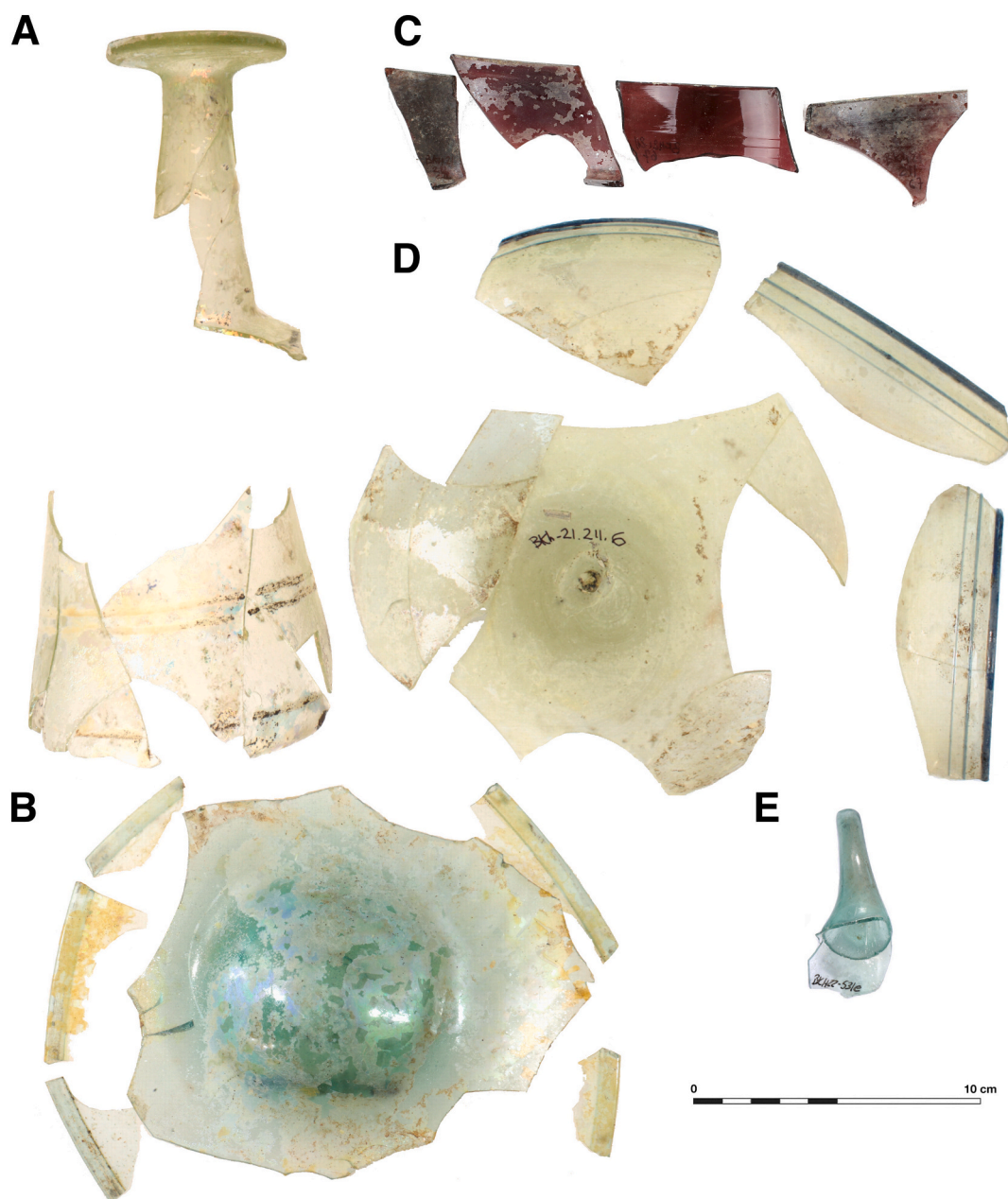


Fig. 3. Examples of glass finds analysed in this study. (a) BKH22 292f (Bukhara-M); (b) BKH22 292v (Bukhara 1a); (c) BKH21 211-67 (Bukhara 1a); (d) BKH21 211-6 (Bukhara 2); (e) BKH22 531e (Bukhara 1b).

important in the Samanid and early Qarakanid period. The glass ingots were included to determine if there was a common Central Asian glass signature.

2.2. LA-ICP-MS

Fresh samples of the glass finds were embedded in epoxy resin and ground to remove any resin and surface alteration. LA-ICP-MS was carried out at IRAMAT-CEB in Orléans (France) as a compositional readout. The analytical setup consists of a Thermo Fischer Scientific ELEMENT XR mass spectrometer in combination with a Resonetics M50E excimer 193 nm laser. A 5 mJ energy and a 10 Hz pulse frequency was used for the analyses, and the diameter of the stationary laser beam was typically 100 μm , occasionally reduced to avoid saturation of the system caused by Mn. After a pre-ablation of 15 s, 58 different isotopes from lithium to uranium were recorded for approximately 27 s, amounting to 9 mass scans for each isotope. The isotopes were selected to minimise possible interferences. An argon/helium flow (1 l/min Ar + 0.65 l/min He) transports the sample material to the plasma torch where it is dissociated, atomised and ionised in the plasma at high temperature (8000 °C). The ions are then separated according to their mass/charge ratios and quantified either with a secondary electron multiplier (SEM) for most ions or the Faraday detector for ^{23}Na , ^{27}Al and ^{39}K (Gratuze, 2016). Two ablations were performed per glass sample unless there were inconsistencies in the spectrum, in which case the analysis was repeated. Silicon is measured in the form of the 28 u isotope (^{28}Si) and used as an internal standard. Background measurements are carried out throughout the analytical sequence and subtracted from each analysis. Five different reference glasses (NIST610, Corning B, C, D and APL1) are used to calculate the response coefficients for each element and to obtain absolute quantitative data (Gratuze, 2016). The calculations are based on an adaptation of the internal standard method previously described (Gratuze, 1999). Assuming that the sum of the different glass constituents is equal or close to 100 %, the following formula can be used to calculate the concentrations of the individual elements detected:

$$\%Y_m O_n = \frac{I_Y \times \alpha_Y}{I_{Si} \times K_Y} \bigg/ \sum \frac{I_X \times \alpha_X}{I_{Si} \times K_X}$$

where I_Y , I_X and I_{Si} are the net intensity count rates corrected for isotopic abundance of isotopes for elements Y, X (all 58 elements) and Si (internal standard). α_Y and α_X are the conversion factors from elements into oxides, while K_Y and K_X are the response coefficient factors according to

$$K_Y = \frac{I_{Y_{std}} \times [\text{Conc}]_{Si_{std}}}{I_{Si_{std}} \times [\text{Conc}]_{Y_{std}}}$$

where $[\text{Conc}]_{Y_{std}}$ and $[\text{Conc}]_{Si_{std}}$ are the concentrations of element Y and Si in the standard material.

To validate the results and to monitor accuracy and precision, standard reference glasses Corning A and NIST 612 were analysed at regular intervals; the difference between certified values and calculated values are given in supplementary Table S3.

2.3. Raman spectroscopy

To investigate the network structure and Q^n speciation of the glass from Bukhara, all but three samples were examined by Raman spectroscopy, using a LabRAM HR Evolution Raman spectrometer (Horiba Jobin Yvon) at the Institut de Physique du Globe de Paris (IPGP). For excitation, a Coherent laser with a wavelength of 488 nm and a nominal laser power of 100 to 400 mW was used. The spectra were acquired with a 50 \times objective and a 50 pinhole in a frequency range between 20 and up to 4000 cm^{-1} , using a grating system of 1800 g/mm. The detection system consists of a charge-coupled multichannel detector (CCD) cooled to -60 °C. The typical acquisition time of a single spectrum was 10–30 s with 3 repetitions. Due to very strong Mn^{2+} fluorescence even at low Mn

concentrations that obscures the Raman signal (Asher and Johnson, 1984; Panczer et al., 2012) an additional laser wavelength in the purple range (405 nm) was used for a sub-set of samples ($n = 26$). The spectra were recorded with an excitation power of 50 mW and a 50 \times objective in the range of 250 to 4000 cm^{-1} . Acquisition time was 60 s with 3 repetitions for each window. This enhanced the Raman spectra while shifting the broad luminescence band of Mn^{2+} to a higher frequency (> 1200 cm^{-1}), thus revealing intense bands in the 850–1200 cm^{-1} range typical of alkali silica glasses (e.g. Mysen et al., 1982; Neuville et al., 2014).

2.4. Treatment of Raman spectra

For comparability, the spectra were corrected for the effects of frequency-dependent scattering using the Long correction (Long, 1977; Neuville and Mysen, 1996):

$$I = I_{\text{obs}} \left\{ \nu_0^3 \left[1 - \exp(-hc\nu/kT) \right] \nu / (\nu_0 - \nu)^4 \right\}$$

where I_{obs} is the measured intensity, h is the Planck constant ($h = 6.62607015 \times 10^{-34}$ Js), k is the Boltzmann constant ($k = 1.3806489 \times 10^{-23}$ J/K), c is the speed of light in vacuum ($c = 299,792,458$ m/s), T is the absolute temperature in [K], ν_0 is the wavenumber of the incident laser (1/487.8 nm = 20,500.2 cm^{-1} ; 1/405 nm = 24,691.4 cm^{-1}), ν is the measured wavenumber in cm^{-1} (Long, 1977; Neuville and Mysen, 1996).

Subsequently, the background was subtracted by defining a spline baseline that was fitted directly to the corrected Raman spectra using MagicPlot Pro 2.9.3. Due to the strong fluorescence of Mn^{2+} , constraining and subtracting the baseline proved to be difficult. As a rule, three to five anchor points were defined along the spectrum in areas devoid of peaks, especially in spectra where the blue laser (488 nm) had been used. It must be conceded that no quantitative information can be extracted from the spectra obtained in this way, but this type of baseline subtraction makes it nonetheless possible to determine the relative degree of polymerisation and distortion of the glass network. Finally, the residual Raman spectra were normalised to the data point with the minimum (I_{min}) and maximum (I_{max}) intensity, using $I_{\text{norm}} = (I - I_{\text{min}}) / I_{\text{max}}$. The spectra were deconvoluted and peaks determined by fitting Gaussian curves according to the procedures provided by Mysen et al. (1982), using again the internal functions of MagicPlot Pro2.9.3.

3. Results

3.1. Base glass compositions

The 71 fragments analysed are all soda-rich plant ash glasses with elevated and highly variable MgO , K_2O and P_2O_5 concentrations. Taking into account both the elements related to the plant ash component and those introduced as part of the silica source, the glass finds can be separated into 5 different production groups (Table 1; Fig. 4). One group (Bukhara-S, $n = 8$) with low sand-related accessory elements such as Al, Ti and Zr along with high MgO (> 4 wt%) and surprisingly low P_2O_5 is an exceptionally clean, colourless glass reminiscent of glass from Samarra (Schibille et al., 2018). A related group of eight samples (Bukhara-M) is not homogeneous and differs from the first group either in terms of the plant ash, reflected in lower ratios of MgO/CaO and somewhat higher P_2O_5 , or in terms of the silica source that is richer in trace and rare earth elements. What these samples have in common are elevated Cr/La ratios (> 5) suggesting a Mesopotamian origin (Schibille, 2022; Schibille et al., 2022). Overall lower trace elements distinguish these two Mesopotamian groups from the other glasses. The difference is particularly pronounced in Rb and Cs, across the REEs, as well as the lower ratios of yttrium to zirconium (Fig. 4). These features are indicative of more mature silica sources compared to the Central Asian glass types. Both Bukhara-S and Bukhara-M groups also have higher chlorine

Table 1
Average composition and standard deviation (σ) of the five different compositional groups identified among the glass finds from Bukhara. Major and minor elements are given as wt% oxides, trace elements in ppm.

	wt%											ppm													
	Na ₂ O	MgO	Al ₂ O ₃	SiO ₂	P ₂ O ₅	Cl	K ₂ O	CaO	Fe ₂ O ₃	Ti	Cr	Mn	Ga	Rb	Sr	Y	Zr	Nb	Ba	La	Ce	Eu	Hf	Th	U
Bukhara-S (n = 8)	12.2	4.94	1.01	71.2	0.09	0.64	2.46	6.53	0.31	272	15.8	3169	1.65	15.3	361	2.94	40.7	1.02	112	3.41	6.34	0.11	1.09	0.94	0.51
σ	0.5	0.23	0.20	0.9	0.02	0.10	0.22	0.17	0.08	52	6.5	739	0.26	1.4	26	0.24	13.0	0.12	33	0.29	0.56	0.02	0.33	0.09	0.09
Bukhara-M (n = 8)	12.9	3.45	1.66	69.1	0.22	0.70	2.91	6.82	1.00	448	46.3	6541	3.47	12.8	339	3.77	45.4	1.46	186	4.54	8.08	0.16	1.17	1.13	0.86
σ	1.6	0.49	0.55	3.0	0.05	0.11	0.75	0.72	0.84	223	32.8	3204	1.44	4.2	82	1.00	30.1	0.43	59	1.79	3.38	0.07	0.70	0.29	0.59
Bukhara 1a (n = 26)	15.1	3.92	4.59	61.5	0.36	0.37	4.63	7.69	0.71	523	11.0	6757	4.75	50.9	499	4.99	40.0	1.79	429	6.66	12.80	0.26	1.06	1.79	1.25
σ	0.8	0.35	0.43	1.3	0.04	0.06	0.36	0.50	0.14	88	2.1	3829	0.35	5.6	104	1.04	6.9	0.33	117	1.18	2.11	0.05	1.07	0.32	0.40
Bukhara 1b (n = 11)	14.6	4.19	2.81	64.4	0.36	0.45	4.18	7.23	0.85	534	13.6	4915	3.59	32.1	528	4.91	42.2	1.76	264	6.56	12.40	0.22	1.09	1.91	1.04
σ	1.0	0.36	0.42	1.8	0.05	0.11	0.30	0.89	0.14	85	2.7	3943	0.67	7.1	311	0.76	7.4	0.27	115	1.09	1.92	0.04	0.19	0.36	0.32
Bukhara 2 (n = 13)	14.6	3.54	4.43	62.8	0.44	0.42	4.96	7.35	0.61	445	9.9	2915	4.77	56.3	509	6.90	35.4	1.62	346	8.23	15.93	0.37	0.93	1.75	1.76
σ	0.5	0.28	0.20	0.8	0.02	0.05	0.24	0.61	0.10	62	1.2	2774	0.40	3.0	44	0.36	3.7	0.21	97	0.58	1.15	0.02	0.11	0.18	1.17

and lower phosphorus contents (Table 1), which points to differences in the plant ash component and its preparation.

The bulk of the assemblage from Bukhara ($n = 50$) has low Cr/La ratios with medium to high, occasionally very high, levels of Al₂O₃ alongside relatively low Ti and Zr concentrations (Fig. 4). The majority of the analysed glass fragments ($n = 39$) have high alumina (Al₂O₃ > 3.5 wt%) and low Ti and Zr that can be further subdivided based on the abundance of REEs relative to Ti and Zr. A group of 26 samples (Bukhara 1a) has lower Y/Zr ratios < 0.15, while a set of 13 samples (Bukhara 2) form a tight and distinct cluster with higher Y/Zr ratios and overall higher REEs in relation to titanium and zirconium (Fig. 4b, c). Several samples are overall consistent with the larger high alumina group (Bukhara 1a) but for their somewhat lower Al₂O₃ (< 3.5 wt%) concentrations. To what extent this is indeed a distinct production group is not entirely clear, because aluminium contents can vary within the same silica source or a glass melt can be poorly mixed (Brems et al., 2018; Freestone et al., 2000). The group was thus named Bukhara 1b. The two subgroups Bukhara 1a and 1b exhibit highly overlapping trace element patterns (Fig. 4c). The exception is a slight positive Eu anomaly of group Bukhara 1a that is most probably linked to the high alumina concentrations of this group and the presence of plagioclase feldspar in the silica source (Weill and Drake, 1973). It can therefore not be considered an independent confirmation of group structures. Hence, the aluminium threshold between Bukhara 1a and Bukhara 1b is a compromise and is introduced first and foremost to allow the demarcation of a more compact cluster (Bukhara 1a).

Three samples from Bukhara (BKH21 211 008, BKH22 411a, BKH22 292a), the two fragments from nearby Paykand and one from Taraz cannot be clearly attributed to any of the main groups and are classified as outliers. A silica source exceptionally rich in accessory minerals underlies the glass chunk from Taraz, reflected in very high Al, Ga, Nb, Hf, Th and U. The sample furthermore shows a marked negative Eu anomaly (Fig. 4c). The two glass chunks from Paykand also display relatively high trace and REE patterns compared to the main glass groups, while the major and minor elements do not differ significantly (Supplementary Table S4; Fig. S1). Sample BKH22 292a is similar to Mesopotamian glass in that it has remarkably high chromium concentrations. However, it also has much higher REEs, while zirconium and hafnium are lower. The remaining two samples (BKH21 211 008, BKH22 411a) are similar but not identical to Bukhara 1 as judged by their higher concentrations in silica-related accessory elements (Supplementary Table S4).

3.2. Colourants / de-colourants

Manganese oxide above the silica-related background levels (MnO > 0.03 wt%) is found in most of the samples from Bukhara, causing strong fluorescence in the form of Mn²⁺ in the Raman spectra. MnO was widely used as decolourant in Roman and Islamic glass to counteract the tinting caused by iron that is naturally present in the silica sources used for ancient glasses. However, the decolouring was not always successful and many of the glass samples that are not intentionally coloured have a bluish or greenish tinge (Supplementary Table S4). The fragments that can be considered truly colourless are the ones belonging to Bukhara-S, which was achieved by the use of exceptionally clean raw materials, since the MnO concentrations are presumably too low to have an effect as decolourant. Colourless are also the samples where MnO clearly outweighs the Fe₂O₃ contents (MnO/Fe₂O₃ > 1.5), with some exceptions in which the absolute iron concentrations remain low (Supplementary Table S4). It is likely that manganese oxide was added to the base glass as part of the general recipe (e.g. Swan et al., 2017). In one sample with a Bukhara 1a base glass (BKH21 211 67), Mn³⁺ (MnO = 1.8 wt%) acts as colourant, producing a purple colour.

Among the vitreous finds there are only a handful of strongly coloured glasses (Supplementary Table S4). The deep blue sample BKH22 531g is coloured by low concentrations of cobalt oxide (0.18 wt%). Copper oxide (0.54 wt%), iron oxide (2.27 wt%) and zinc (434 ppm) are

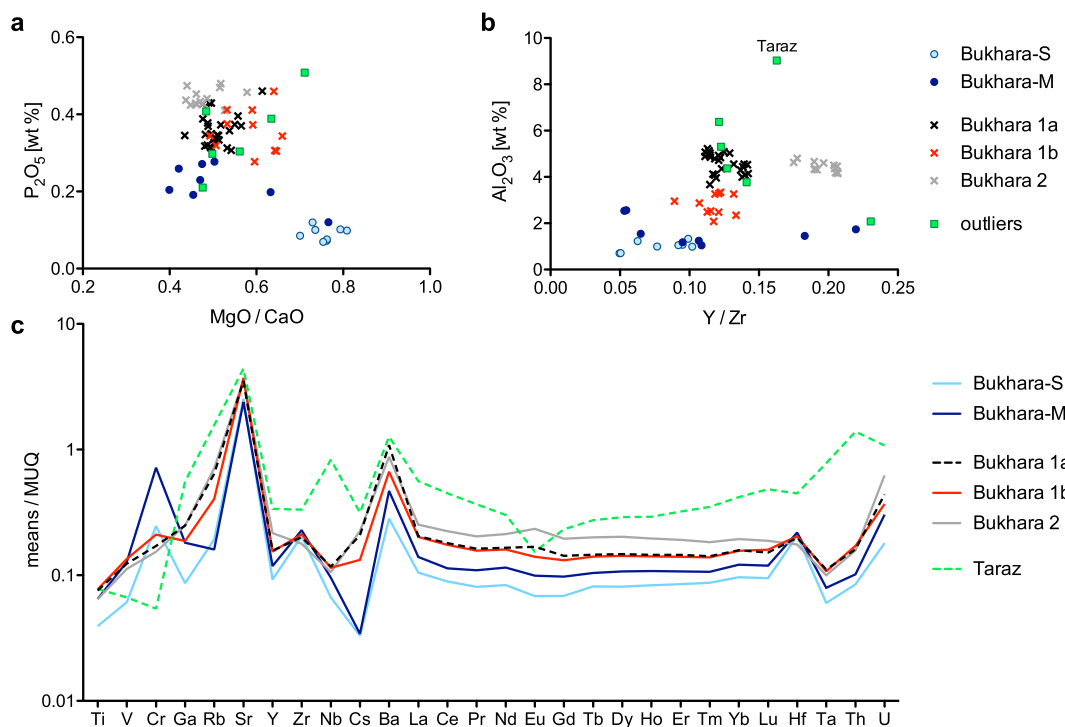


Fig. 4. Base glass characteristics of the five compositional groups and outliers identified at Bukhara. (a) MgO/CaO versus P_2O_5 showcases differences in the plant ash component between the imported Bukhara-S, Bukhara-M and the local Bukhara 1 and 2 groups; (b) Y/Zr and Al_2O_3 contents differentiate the five glass groups according to the silica source; (c) average trace element profiles of the different groups normalised to the upper continental crust (MUQ, Kamber et al., 2005) highlight similarities between Bukhara 1a, 1b and 2, while separating the Bukhara-S and Bukhara-M glass.

elevated along with the cobalt, suggesting that the cobalt source used was also enriched in these components. Only two other samples have notable cobalt contents (Co > 180 ppm), one of which (BKH22 110) has even higher zinc concentrations relative to cobalt and copper, while the other (BKH22 337f) has also relatively high nickel contents (325 ppm). All three fragments belong to the high Cr/La Bukhara-M group. The differences in the cobalt signature reinforce the heterogeneity of this group both in terms of the base glass and the colouring compounds.

Two bluish turquoise fragments (BKH21 211 13; BKH22 292j) are coloured by dissolved copper oxide ($CuO \geq 1$ wt%). In both samples, arsenic, tin, antimony and lead are more or less elevated, which may reflect specific copper sources and/or colouring techniques. Both specimens are part of the Bukhara 2 base glass group. About a third of the analysed glass samples ($n = 26$) have CuO and/or PbO above the usual background levels (> 100 ppm), indicating that they may have been subject to recycling and that some coloured cullet was added to the batch (Fig. S2). This applies to all raw glass groups equally, with the exception of the Bukhara-S samples, which show no signs of recycling (except bottle BKH22 337e).

3.3. Raman spectra and the degree of polymerisation

Silica glass is composed of tetrahedral units so-called Q^n where n represents the number of bridging oxygens bonded covalently to a silicon atom. In pure silica glass, these oxygen atoms are typically shared with another silicon atom as bridging oxygens (BO) to form a three-dimensional network of Q^4 species with Si-O-Si bonding. These connections can be broken by the addition of other chemical elements such as alkali, alkali earth or transition elements that form non-bridging oxygens (NBO) bound to only one silicon atom, resulting in a mixture of different Q^n -species, where n (0–4) is the number of BOs. Raman spectra are a good probe to investigate this organisation and connectivity of the glass network and its Q^n speciation (Neuville et al., 2014).

The relevant range (10 to 1400 cm^{-1}) can be divided into four

sections: the Boson region (10–250 cm^{-1}); the low frequency region (250–700 cm^{-1}); the medium frequency region (700–850 cm^{-1}); the high frequency region 850–1300 cm^{-1} . Below 250 cm^{-1} , there is a scattering continuum and the Raleigh tail of the excitation line, except at very low frequency where there is the so-called Boson peak (Buchenau et al., 1986; Malinovsky and Sokolov, 1986). This peak is attributed to excitations associated with rotational motions of nearly rigid tetrahedra (Buchenau et al., 1986; Neuville, 2006). The peak is eliminated by the Long correction and baseline subtraction, but is clearly visible in the raw spectral data. Its exact peak position and shape appear to depend on the polymerisation and the silica content of the glass as well as the nature of the network modifier (e.g. Le Losq et al., 2014; Neuville, 2006). In the glass from Bukhara, the variation of the frequency of the Boson peak around 65 cm^{-1} is very small because the silica content is relatively stable between 65 and 75 wt%. There is nonetheless a tendency towards higher frequencies of the Boson peak in Bukhara 1 and 2 compared to the samples that were imported from Mesopotamia. This observation is in agreement with the higher concentrations of network modifiers and a stronger distortion of the SiO_4 tetrahedra in Bukhara 1 and Bukhara 2.

The Raman spectrum above 500 cm^{-1} is primarily due to vibrations of the Si-O network with the modifiers essentially at rest (Phillips, 1984). Recently, Hehlen and Neuville (2020) have shown that the peak near 400 cm^{-1} can also be attributed to alkali or alkaline earth elements as network modifiers. This area is still very controversial and beyond the scope of the present article. The peak near 580 cm^{-1} visible in Bukhara-S and Bukhara-M samples is related to the $Si-O^0$ rocking motions of fully polymerised Q^4 units (Fig. 5). Bukhara 1 and 2, on the other hand, show peaks at 600–615 cm^{-1} indicative of Si-O-Si bending vibrations in less polymerised structural units (Neuville et al., 2014; Yadav and Singh, 2015). The difference most likely reflects, among other things, the higher Na_2O / MgO ratios in Bukhara 1 and 2 compared to the Bukhara-S compositions (Fig. S3; see, e.g. Neuville et al., 2022).

In simple glass compositions such as silicate glass, the broad peak at 800 cm^{-1} is sensitive to the size of the cation and generally shifts to

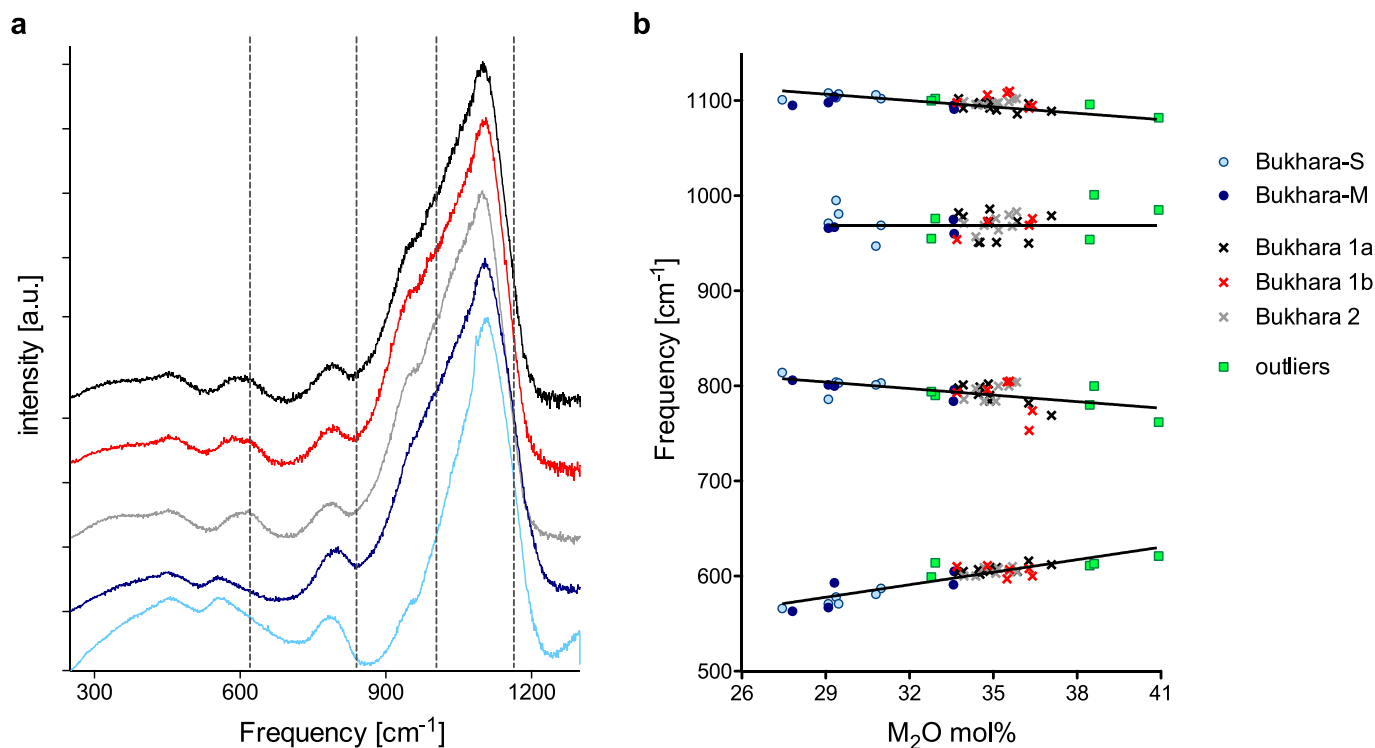


Fig. 5. Raman spectra for the different compositional groups from Bukhara. (a) Corrected, baseline subtracted and normalised spectra of the representative samples BKH22 531 (Bukhara-S), BKH21 211 37 (Bukhara-M), BKH21 211 09 (Bukhara 1a), BKH22 531h (Bukhara 1b) and BKH22 531k (Bukhara 2); (b) frequencies of deconvoluted Raman bands as a function of the sum of M_2O contents ($M = Li, Na, K, Ca/2, Mg/2, Sr/2, Ba/2$), separated according to the compositional groups. The lines show linear regressions of the data points.

higher frequencies as the size of the cation increases (e.g. Le Losq et al., 2014; Neuville, 2006). It appears to be associated with asymmetric stretching vibrations of bridging oxygens between tetrahedra (Le Losq et al., 2014; Neuville et al., 2014). The Bukhara-S and Bukhara-M samples tend to show a band near 800 cm^{-1} that is shifted to lower frequencies in the Bukhara 1 and 2 glasses (Fig. 5b). This would seem to imply that in complex vitreous systems, this band is shifted to lower frequencies with increasing modifiers.

The most important structural information can be gleaned from the T-O-T stretching vibrations in the high frequency domain ($850\text{--}1200\text{ cm}^{-1}$), where T can be Si, Al, Fe, or Ti (Neuville et al., 2014; Neuville et al., 2022). An intense broad band near 1100 cm^{-1} is due to Si-O stretching vibrations in Q^3 units, which is in good agreement with the SiO_2 content close to 70 wt% (Le Losq et al., 2014; Mysen, 1997; Mysen et al., 1982; Neuville et al., 2014). In the Bukhara-S samples, this band is ever so slightly shifted to higher frequencies ($> 1100\text{ cm}^{-1}$), possibly indicating a small proportion of Q^4 units (Mysen et al., 1982). There is no clear trend in the range between 940 cm^{-1} and 1000 cm^{-1} that most likely corresponds to the Si-O stretching in Q^2 units with two non-bridging oxygens (Mysen and Frantz, 1994; Neuville et al., 2014). The shoulder near 980 cm^{-1} may be caused by Fe^{3+} in four-fold coordination (Cochain et al., 2012; Magnien et al., 2006), Ti^{4+} in five-fold coordination (Mysen and Neuville, 1995), SO_4^{2-} (Lenoir et al., 2009) or CO_2 (Amalberti et al., 2021).

Taken together, the spectral features indicate subtle differences between the groups identified based on the chemical composition. The position of the band in the low frequency envelop ($550\text{--}650\text{ cm}^{-1}$) shifts to higher frequencies with increasing M_2O , while the various bands in the high frequency range ($800\text{--}1150\text{ cm}^{-1}$) tend to decrease in frequency with increasing M_2O (Fig. 5b). Both trends appear to confirm a growing depolymerisation of the silicate network and reduction in connectivity in the Central Asian glasses from Bukhara. It can be assumed that these differences have an effect on the viscosity and glass

transition temperature of the different compositional groups, with the Bukhara groups tending to have a lower glass transition temperature.

4. Discussion

4.1. Comparison of the compositional data with potential source areas

In the 10th century, primary glassmaking was practised throughout the Islamic world, including Mesopotamia, Khorasan and Mawarannahar (*mā warāʿ-al-nahr* – “that which is beyond the river”) (Chinni et al., 2023; Schibille, 2022; Schibille et al., 2022). In Mawarannahar this was in fact an important cultural innovation, because glass had been extremely rare in the region during previous periods (Raspopova, 2011). Archaeological evidence of glass production sites in Central Asia during the early Islamic period is severely limited. Only from the town of Paykand is there clear archaeological evidence for the presence of a glass workshop, although this was never properly published (Naimark, 1985), and a possible furnace for glass processing from the late Qarakhanid period was reported from the southern suburbs of Bukhara (Nekrasova, 2011). We therefore have to resort to the chemical composition of the glass itself. The likely provenance of the glass from Bukhara can be assessed on the basis of the base glass characteristics in comparison with the available database of glass compositions from across the early Islamic world. By tracking the distribution of a particular glass type in regional assemblages in addition to the observed degree of recycling, conclusions can be drawn about putative primary production sites and the direction of exchange.

If we compare the glass groups from Bukhara with published data from Mesopotamian and Central Asian sites, we find that a large proportion of the glass does not have close parallels anywhere else. In other words, the Bukhara 1 and 2 glasses are probably from Central Asia and more specifically probably from the region around Bukhara itself. These glasses can thus be considered new regional production groups,

manufactured using the available raw materials. Exceptions to this pattern are the Bukhara-S and Bukhara-M glasses that were traded over long distances (up to 2500 km) from the Euphrates and Tigris river valleys all the way to the Bukhara oasis (Fig. 1). As many as 22 % of the analysed objects can be classified as Bukhara-S or Bukhara-M glass, including all the wheel-cut and cobalt blue fragments. The samples belonging to the Bukhara-S group fall within the compositional limits of Samarra 1 (Schibille et al., 2018) across the entire range of trace and rare earth elements (Fig. 6a). One sample (BKH22 337d) is also topologically very similar to a fragment from Samarra (Fig. 7). Based on our data, we can therefore conclude that these 8 samples most likely originated from the vicinity of the 9th-century Abbasid capital on the east bank of the Tigris river.

Bukhara-M data do not match the Samarra glass, with disparities evident especially for the Ti/Zr ratios and across the REEs (Fig. 6a). As a group, Bukhara-M is highly heterogenous, indicating different primary

production events and by implication different production sites. Nonetheless, the data exhibit a relatively good match with Sasanian glass from Veh Ardashir (Ganio et al., 2013; Mirti et al., 2009; Mirti et al., 2008) for practically all trace elements (Fig. 6a). To more tightly constrain the possible source areas of these glasses, further careful sampling and analysis of Mesopotamian glass, both Sasanian and early Islamic, will be necessary. Given the variability of compositions, the typological similarities with Mesopotamian glass assemblages and the compositional specificity of cobalt glass, it can be surmised that these glasses travelled as finished products. Their presence in Bukhara reflects in part the economic and cultural value of these objects, and in part perhaps the technical and/or material limitations of Central Asian glass production at the time.

To determine the most likely source area for the Bukhara 1 and Bukhara 2 groups, we compared their aluminium and trace element signatures to data of contemporary glass assemblages from Merv,

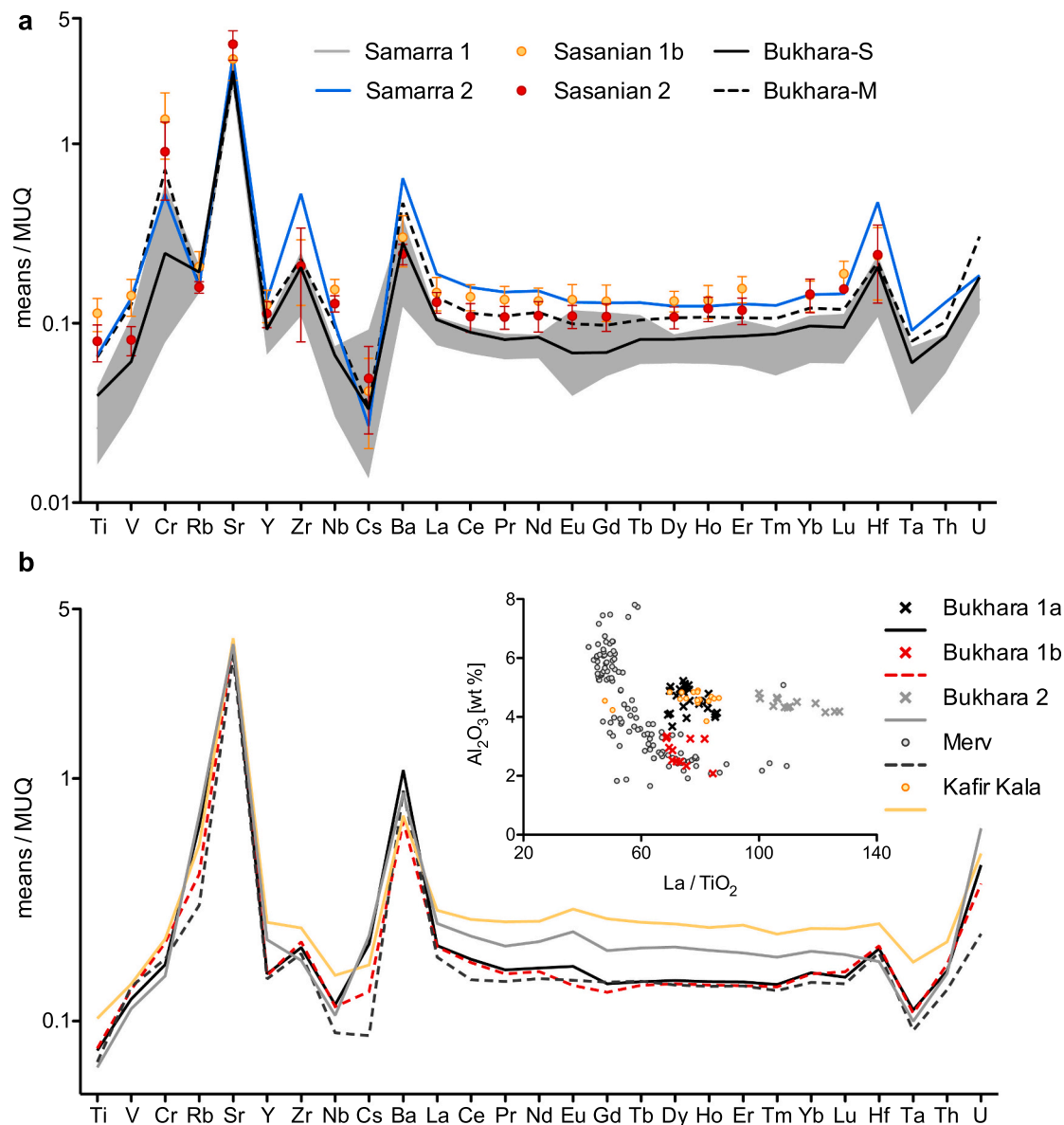


Fig. 6. Comparison of average trace element profiles of the Bukhara compositional groups with reference material. (a) Bukhara-S and Bukhara-M profiles compared to data from Samarra (Schibille et al., 2018) and Veh Ardashir (Mirti et al., 2009; Mirti et al., 2008). The shaded area corresponds to the range of Samarra 1 compositions, while the Sasanian glass from Veh Ardashir are given as averages with standard deviations; (b) trace elements of Bukhara 1a, 1b and 2 compared to an assemblage from Karif-Kala near Samarkand (Chinni et al., 2023) and a subgroup from Merv with moderate aluminium levels (Schibille, 2022). Inset shows that the majority of the glass from Merv has very different characteristics related to the silica source.

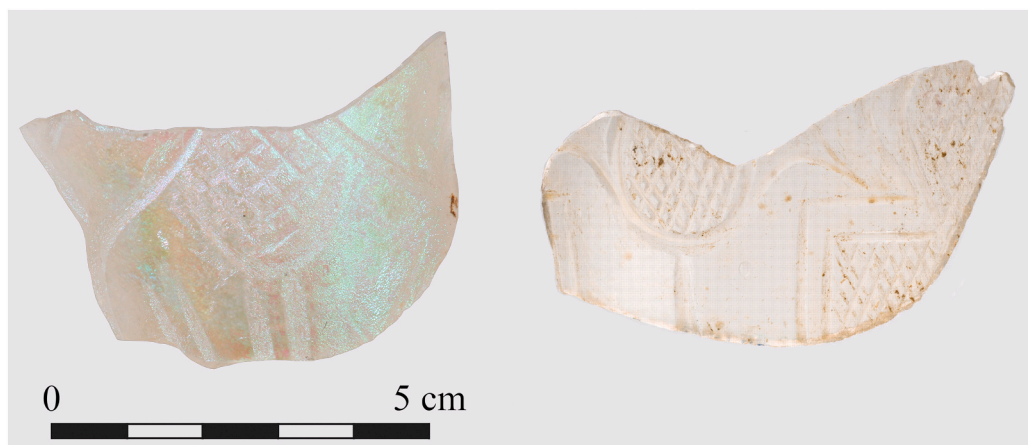


Fig. 7. Sample BKH 22-337d (left) from Bukhara with a Samarra base glass compared to fragment with similar wheel cut decoration from Samarra (Id Sam I. 45). © Staatliche Museen zu Berlin, Museum für Islamische Kunst / Christian Krug).

Turkmenistan about 360 km to the west (Schibille, 2022), and the citadel of Kafir-Kala near Samarkand about 300 km east of Bukhara (Chinni et al., 2023). The recently described compositional groups from Gorgan in Iran could be excluded because of the deviating trace element profiles, particularly their considerably higher Ti, Zr or Hf concentrations (Schibille et al., 2022). The majority of samples from Merv (Schibille, 2022) can likewise be discarded as an acceptable match due to their higher zirconium and/or titanium contents and resulting lower La/TiO₂ ratios (Fig. 6b). However, a small subset of the Merv samples have moderate aluminium levels and yields a potential match for Bukhara 1b both in terms of the plant ash as well as the silica source. All the trace elements of these Merv samples lie within the perimeters of the Bukhara 1b data (Fig. 6b). The difference pertains to the concentrations of additives such as copper and lead, possible indicators of recycling, which are generally higher in the glass finds from Merv. Similarly, some glass finds from Kafir-Kala (group B, Chinni et al., 2023) are compatible with Bukhara 1 and Bukhara 2 in terms of most major, minor and trace elements, except for their higher REEs even compared to Bukhara 2 (Fig. 6b). The glass from Kafir-Kala has practically no manganese above normal background levels and surprisingly high antimony oxide concentrations (0.22 wt%), for which there is no precedent in early Islamic glass production. These differences therefore rule out a direct link between the glass assemblages from Bukhara and Kafir-Kala, especially if we assume that manganese was added at the primary production stage (e.g. Swan et al., 2017).

The geochemical similarities between Bukhara 1 and the subgroup from Merv and the glass from Kafir Kala reflect compositional patterns that suggest a Central Asian origin. Since no perfect compositional match was found for either Bukhara 1 or for Bukhara 2, and assuming that recycling increases with distance from the source, we propose that the region around Bukhara was the probable production area of Bukhara 1 and possibly of Bukhara 2. Of the 47 samples belonging to Bukhara 1 and Bukhara 2 that have not been intentionally coloured, about half show no clear signs of recycling, and both copper and lead contents remain low (< 100 ppm). Last not least, architectural glass in the form of window fragments was found among both the Bukhara 1 and Bukhara 2 groups, further suggesting a local production.

4.2. Compositional characteristics of early Islamic glass from Central Asia

All the glass finds analysed in this study date to the 10th and early 11th centuries, when Bukhara hosted a court of supra-regional importance, first for the Samanid dynasty after Ismail b. Ahmad had risen to political seniority within the Samanid family in 892/3 CE, and then for the Qarakhanid dynasty from 999 CE. This was a time of industrial and commercial prosperity in the regions of Khorasan and Mawarannahar

(Bosworth, 1995; Davidovich, 1966; Mal'tsev, 1982; Negmatov, 1977). Local production of the famous Samanid slipware in Bukhara is also well documented (supplementary table S1), so glass production around the capital may therefore not be entirely unexpected. If glass had exclusively been imported, the same glass groups should be found as in other contemporary contexts. As it stands, the Bukhara assemblage is characterised by a relatively low complexity, with two new and likely locally produced glass types making up the bulk of the finds. Bukhara 1 and Bukhara 2 have significantly higher aluminium, strontium, barium and REEs in comparison to Mesopotamian glass, while titanium, zirconium and hafnium are proportionally lower. The compositional characteristics of Bukhara 1 and Bukhara 2 are fully consistent with a local glass production that exploited a nearby silica source more or less enriched in aluminosilicate minerals.

It seems that Bukhara 1 and Bukhara 2 were not traded over long distances, which argues for a production model on a small, local scale. The differences evident in the glass finds from Merv and Kafir-Kala (Samarkand), in relative geographical proximity, also indicate a multiplication and dispersion of glass workshops in the Islamic east. It can thus be inferred that the glass most commonly used for everyday objects and architectural glass in the Samanid period came from the immediate vicinity of the respective urban centres (e.g. Bukhara, Samarkand, Merv). Larger quantities of glass cannot be easily transported overland, which limits economic viability. However, there was long distance trade of some glass objects, possibly related to technological limitations, lack of raw materials (e.g. cobalt) and/or know-how (use of pure silica sources). For example, the exceptionally clean and colourless glass from Samarra (Samarra 1) has been imported to Bukhara in the form of finely crafted objects. Similarly, all cobalt blue fragments are of Mesopotamian origin. These patterns of selective procurement can also be observed in other places such as Nishapur and Merv (Schibille, 2022; Schibille et al., 2022). There is no satisfactory explanation for the production and use of two different local glass compositions in the form of Bukhara 1 and Bukhara 2. No pattern in the type of objects seems to be connected to the different base glass groups, with free-blown and mould-blown bowls, bottles, and vials being part of both groups. The only observed difference between Bukhara 1 and 2 is in the presence of alembics, which are constrained to Bukhara 1. Perhaps this is simply another indication of the small scale of production and batch sizes or a slightly different production date of Bukhara 1 and Bukhara 2 glass.

Variations in the glass network structure determined by Raman spectroscopy confirm the compositional classifications that may point to systematic differences in the technology and/or raw materials between Mesopotamian and Central Asian glassmaking. Bukhara-S and for the most part also Bukhara-M glass appear to have a higher proportion of fully polymerised SiO₄ tetrahedral units than Bukhara 1 and 2. This has

an impact on the network connectivity that appears more strongly modified in the groups produced in Bukhara compared to the glass imported from Samarra and Mesopotamia. The implications of this are far from understood in multicomponent silica glasses, where the attribution of peaks to specific structural features becomes increasingly complex due to overlaps and cation substitution of alkali and alkaline earth elements (Drewitt et al., 2022; Neuville et al., 2022). It can be assumed that these structural variations, even if minimal, will affect the molar volumes and viscosity (Fig. S4), and thus the glass transition temperature. A lower working temperature in turn affects fuel requirements and/or furnace configuration. Further work is required to gain a better understanding of the effects of complex glass compositions on the structural organisation of the glass and the role of individual elements within the glass network. The potential function of magnesium as network former may be relevant, as Sasanian and Islamic glass produced in Mesopotamia is characterised by exceptionally high MgO concentrations. Here, especially bands in the low to medium frequency region of the Raman spectrum, which show the clearest shifts, may shed further light on the technological specificities of Mesopotamian glass in direct comparison with other regional production groups.

5. Conclusion

To summarise, the Bukhara glass assemblage consists of at least five compositional groups, two of which are probably Mesopotamian and three of likely Central Asian origin. The Central Asian types represent local or at least regional production groups, while high-end Samarra glass and some Mesopotamian artefacts, including all cobalt coloured finds, most likely travelled along the Silk Roads from the Euphrates and Tigris river plain as finished objects. Early Islamic glass coloured with cobalt generally appears to be of a predominantly Mesopotamian signature regardless of the find spot, indicating possible sources of cobalt in western Iran. Judging from the data currently available, glass from Central Asia has higher levels of mineral impurities related to the silica source compared to Mesopotamian and Mediterranean glass, especially as regards aluminium and REEs in relation to Ti and Zr. The glasses also show differences in the plant ash composition such as phosphorus, chlorine and potassium, as well as in the network structure and degree of polymerisation. Taken together, this indicates differences in both the raw materials and the production technique. Whether this may be a legacy of Sasanian glassmaking or whether the production of glass was only introduced after the Arab conquest is currently not clear. Either way, the sudden surge of glass production in Mawarannahr after the Arab conquest must be seen against the backdrop of the specific historical conditions under which the conquest and subsequent cultural changes took place. As in other areas of material culture (e.g. artistic metalware, Marschak, 1986), Khorasani *mawālī*, who came to Mawarannahr with the Arab conquerors as administrators may have played a decisive role in the introduction of elite tastes and forms of expression that were new to Mawarannahr but already common in Sasanian Iran-shahr. Perhaps the emerging taste for glassware in Mawarannahr was originally popularised by this class of new Persian speaking administrators, possibly with the assistance of Khorasani masters trained in Sasanian glassmaking.

CRedit authorship contribution statement

Nadine Schibille: Conceptualization, Validation, Formal analysis, Investigation, Visualization, Writing- original draft; revisions.

Catherine Klesner: Conceptualization, Investigation, Writing- original draft, revisions.

Daniel Neuville: Methodology, Validation, Resources, Writing- original draft, revisions.

Sören Stark: Acquisition of Archaeological Data, Conceptualization, Resources, Writing- original draft, Illustrations, Funding acquisition, revisions.

Asan I. Torgoev: Acquisition of Archaeological Data.

Sirojiddin J. Mirzaakhmedov: Acquisition of Archaeological Data.

Declaration of competing interest

The authors declare that they have no known competing financial interests or personal relationships that could have appeared to influence the work reported in this paper.

Acknowledgements

We would like to thank all participants of the 2021 and 2022 Bukhara excavations seasons in the Shakhristan area, in particular Dilmurod Kholov, Vikentiy Parshuto, Husniddin Rakhmanov, Emily Everest-Phillips, Tianrui Zhu, and Lauren Morris. Thanks are also due to Adrien Donatini at the IGP for his help with the Raman spectroscopy.

Funding

This work was supported by a grant from the Max-van-Berchem Foundation and the Rust Family Foundation.

Appendix A. Supplementary data

Supplementary data to this article can be found online at <https://doi.org/10.1016/j.chemer.2024.126078>.

References

- Abdurazakov, A.A., 1998. Steklodelatel'noe remeslo v srednevekovoi Bukhare. *Obshchestvennye nauki v Uzbekistane* 4-5, 51–54.
- Amalberti, J., Sarda, P., Le Losq, C., Sator, N., Hammouda, T., Chamorro-Pérez, E., Guillot, B., Le Floch, S., Neuville, D.R., 2021. Raman spectroscopy to determine CO₂ solubility in mafic silicate melts at high pressure: Haplobasaltic, haploandesitic and approach of basaltic compositions. *Chem. Geol.* 582, 120413.
- Anarbaev, A., 1981. Благоустройство средневекового города Средней Азии (V-XIII в.) / Development of Medieval Cities in Central Asia (5th–13th Centuries). Fan, Tashkent.
- Asher, S.A., Johnson, C.R., 1984. Raman spectroscopy of a coal liquid shows that fluorescence interference is minimized with ultraviolet excitation. *Science* 225, 311–313.
- Bosworth, C.E., 1995. Samanids 1: history, literary life and economic activity. In: *The Encyclopedia of Islam*. New Edition. Brill, Leiden, pp. 1026–1029.
- Brems, D., Freestone, I.C., Gorin-Rosen, Y., Scott, R., Devulder, V., Vanhaecke, F., Degryse, P., 2018. Characterisation of Byzantine and early Islamic primary tank furnace glass. *J. Archaeol. Sci. Rep.* 20, 722–735.
- Buchenau, U., Prager, M., Nücker, N., Dianoux, A., Ahmad, N., Phillips, W., 1986. Low-frequency modes in vitreous silica. *Phys. Rev. B* 34, 5665.
- Chinni, T., Fiorentino, S., Silvestri, A., Mantellini, S., Berdimuradov, A.E., Vandini, M., 2023. Glass from the Silk Roads. Insights into new finds from Uzbekistan. *J. Archaeol. Sci. Rep.* 48, 103841.
- Cochain, B., Neuville, D., Henderson, G., McCammon, C., Pinet, O., Richet, P., 2012. Effects of the iron content and redox state on the structure of sodium borosilicate glasses: a Raman, Mössbauer and boron K-edge XANES spectroscopy study. *J. Am. Ceram. Soc.* 95, 962–971.
- Davidovich, E.A., 1966. Denejnoe obrashchenie v Mawarannakhre pri Samanidakh. *Numizmatika i epigrafika* 6, 103–134.
- Drewitt, J.W., Hennet, L., Neuville, D.R., 2022. From short to medium range order in glasses and melts by diffraction and Raman spectroscopy. *Rev. Mineral. Geochem.* 87, 55–103.
- Freestone, I.C., Gorin-Rosen, Y., Hughes, M.J., 2000. Primary glass from Israel and the production of glass in late antiquity and the Early Islamic period. In: Nenna, M.-D. (Ed.), *La Route du verre. Ateliers primaires et secondaires du second millénaire av. J.-C. au Moyen Âge*. Colloque organisé en 1989 par l'Association française pour l'Archéologie du Verre (AFAV). Maison de l'Orient et de la Méditerranée, Lyon, pp. 65–83.
- Ganio, M., Gulmini, M., Latruwe, K., Vanhaecke, F., Degryse, P., 2013. Sasanian glass from Veh Ardašir investigated by strontium and neodymium isotopic analysis. *J. Archaeol. Sci.* 40, 4264–4270.
- Giordano, D., González-García, D., Russel, J.K., Raneri, S., Bersani, D., Fornasini, L., De Genova, D., Ferrando, S., Kaliwoda, M., Lottici, P.P., Smit, M., Dingwell, D.B., 2019. A calibrated database of Raman spectra for natural silicate glasses: implications for modelling melt physical properties. *J. Raman Spectrosc. Special Issue*, 1–17.
- Gratuzé, B., 1999. Obsidian characterization by laser ablation ICP-MS and its application to prehistoric trade in the Mediterranean and the near east: sources and distribution of obsidian within the Aegean and Anatolia. *J. Archaeol. Sci.* 26, 869–881.
- Gratuzé, B., 2016. Glass characterization using laser ablation-inductively coupled plasma-mass spectrometry methods. In: Dussubieux, L., Goltko, M., Gratuzé, B.

- (Eds.), Recent Advances in Laser Ablation ICP-MS for Archaeology, Series: Natural Science in Archaeology. Springer, Berlin, Heidelberg, pp. 179–196.
- Hehlen, B., Neuville, D.R., 2020. Non network-former cations in oxide glasses spotted by Raman scattering. *Physical Chemistry Chemical Physics* 22, 12724–12731.
- Henderson, J., Chenery, S., Faber, E., Kröger, J., 2016. The use of electron probe microanalysis and laser ablation-inductively coupled plasma-mass spectrometry for the investigation of 8th–14th century plant ash glasses from the Middle East. *Microchem. J.* 128, 134–152.
- Henderson, J., Ma, H., Evans, J., 2020. Glass production for the Silk Road? Provenance and trade of Islamic glasses using isotopic and chemical analyses in a geological context. *J. Archaeol. Sci.* 119, 105164.
- Kamber, B.S., Greig, A., Collerson, K.D., 2005. A new estimate for the composition of weathered young upper continental crust from alluvial sediments, Queensland, Australia. *Geochim. Cosmochim. Acta* 69, 1041–1058.
- Kröger, J., 1995. *Nishapur: Glass of the Early Islamic Period*. Metropolitan Museum of Art, New York.
- Le Losq, C., Neuville, D.R., Florian, P., Henderson, G.S., Massiot, D., 2014. The role of Al³⁺ on rheology and structural changes in sodium silicate and aluminosilicate glasses and melts. *Geochim. Cosmochim. Acta* 126, 495–517.
- Lenoir, M., Grandjean, A., Poissonnet, S., Neuville, D., 2009. Quantitation of sulfate solubility in borosilicate glasses using Raman spectroscopy. *J. Non Cryst. Solids* 355, 1468–1473.
- Long, D.A., 1977. *Raman Spectroscopy*. McGraw-Hill, New York.
- Magnien, V., Neuville, D., Cormier, L., Roux, J., Hazemann, J.-L., Pinet, O., Richet, P., 2006. Kinetics of iron redox reactions in silicate liquids: a high-temperature X-ray absorption and Raman spectroscopy study. *J. Nucl. Mater.* 352, 190–195.
- Mal'tsev, I.S., 1982. *Maverannakhr i ego torgovo-ekonomicheskii potentsial v epokhu Samanidov: po svedeniiam anonimnogo traktata X v. 'Khudud-al-alam'*. Izvestiia Akademii Nauk Tadzhikskoi SSR, Otdelenie obschestvennykh nauk 2, pp. 90–97.
- Malinovsky, V.K., Sokolov, A.P., 1986. The nature of boson peak in Raman scattering in glasses. *Solid State Commun.* 57, 757–761.
- Marschak, B.I., 1986. *Silberschätze des Orients. Metallkunst des 3. - 13. Jahrhunderts und ihre Kontinuität*. E. A. Seemann Verlag, Leipzig.
- Mir-Makhamad, B., Stark, S., Mirzaakhmedov, S., Rahmonov, H., Spengler III, R.N., 2023. Food globalization in southern Central Asia: archaeobotany at Bukhara between antiquity and the Middle Ages. *Archaeol. Anthropol. Sci.* 15, 124.
- Mirti, P., Pace, M., Negro Ponzi, M.M., Aceto, M., 2008. ICP-MS analysis of glass fragments of Parthian and Sasanian epoch from Seleucia and Veh Ardasir (Central Iraq). *Archaeometry* 50, 429–450.
- Mirti, P., Pace, M., Malandrino, M., Negro Ponzi, M., 2009. Sasanian glass from Veh Ardasir: new evidences by ICP-MS analysis. *J. Archaeol. Sci.* 36, 1061–1069.
- Mirzaakhmedov, D.K., Stark, S., Torgoev, A.I., Mirzaakhmedov, S.D., Rakhmanov, Kh.U., Kholov, D.O., Moris, L., Parshuto, V.A., 2023. Novye materialy po istoricheskoi topografii vnutrennego goroda Bukhary v antichnosti i srednevekov'e (po materialam rabot 2020–2022 gg.). *Arkheologicheskie Issledovaniia v Uzbekistane* 15, 138–144.
- Mysen, B., 1997. Aluminosilicate melts: structure, composition and temperature. *Contrib. Mineral. Petr.* 127, 104–118.
- Mysen, B., Frantz, J., 1994. Silicate melts at magmatic temperatures: in-situ structure determination to 1651 C and effect of temperature and bulk composition on the mixing behavior of structural units. *Contrib. Mineral. Petr.* 117, 1–14.
- Mysen, B., Neuville, D., 1995. Effect of temperature and TiO₂ content on the structure of Na₂Si₂O₅-Na₂Ti₂O₅ melts and glasses. *Geochim. Cosmochim. Acta* 59, 325–342.
- Mysen, B.O., Finger, L.W., Virgo, D., Seifert, F.A., 1982. Curve-fitting of Raman spectra of silicate glasses. *Am. Mineral.* 67, 686–695.
- Naimark, A.I., 1985. *Otchët a rabotakh Paikenskogo otriada GMINV v 1984 g. Otchët ob arkheologicheskikh issledovaniiax Paikenskogo otriada v 1984 g* (unpublished field report, Archive of the Archaeological Institute Samarkand, Call No. 2.1.6255). Samarkand, pp. 41–66.
- Narshakhī, A.B.M.J., 1954. *The History of Bukhara*. trans. R.N. Frye.. The Medieval Academy of America, Cambridge, Mass.
- Negmatov, N.N., 1977. *Gosudarstvo Samanidov (Maverannakhr i Khorasan v IX-X vv.)*. Donish, Dushanbe.
- Nekrasova, E.G., 2011. *Arkheologo-topograficheskii komentarii*. In: an-Narshakhi, M. (Ed.), *Ta'rikh-i Bukhara – Istoriia Bukhary*. SMI-ASIA, Tashkent, pp. 441–509.
- Neuville, D.R., 2006. Viscosity, structure and mixing in (Ca, Na) silicate melts. *Chem. Geol.* 229, 28–41.
- Neuville, D.R., Henderson, G.S., Dingwell, D.B., 2022. Geological Melt. *Rev. Mineral. Geochem.* 87, 105–162.
- Neuville, D.R., Mysen, B.O., 1996. Role of aluminium in the silicate network: in situ, high-temperature study of glasses and melts on the join SiO₂-NaAlO₂. *Geochim. Cosmochim. Acta* 60, 1727–1737.
- Neuville, D.R., De Ligny, D., Henderson, G.S., 2014. Advances in Raman spectroscopy applied to earth and material sciences. *Rev. Mineral. Geochem.* 78, 509–541.
- Panczer, G., De Ligny, D., Mendoza, C., Gaft, M., Seydoux-Guillaume, A.-M., Wang, X., Dubessy, J., Caumon, M., Rull, F., 2012. Raman and fluorescence. *EMU Notes in Mineralogy* 12, 61–82.
- Phelps, M., 2018. Glass supply and trade in early Islamic Ramla: An investigation of the plant ash glass. In: Rosenow, D., Phelps, M., Meek, A., Freestone, I.C. (Eds.), *Things that Travelled: Mediterranean Glass in the First Millennium CE*. UCL Press, London, pp. 236–282.
- Phillips, J., 1984. Microscopic origin of anomalously narrow Raman lines in network glasses. *J. Non Cryst. Solids* 63, 347–355.
- Raspopova, V.I., 2011. *Stekliannye sosudy iz Pendjikenta (nakhodki 1950–1999 gg.)*. Sintez buk, Sankt-Peterburg.
- Schibille, N., 2022. *Islamic Glass in the Making: Chronological and Geographical Dimensions*. Leuven University Press, Leuven.
- Schibille, N., Meek, A., Wypyski, M.T., Kröger, J., Rosser-Owen, M., Haddon, R.W., 2018. The glass walls of Samarra (Iraq): ninth-century Abbasid glass production and imports. *PLoS One* 13, e0201749.
- Schibille, N., Lankton, J., Gratuze, B., 2022. Compositions of early Islamic glass along the Iranian Silk Road. *Geochemistry* 125903.
- Stark, S., 2018. The Arab conquest of Bukhara: reconsidering Qutayba b. Muslim's campaigns 87–90 H/706–709 CE. *Der Islam* 95, 367–400.
- Stark, S., Kidd, F., Mirzaakhmedov, D., Silvia, Z., Mirzaakhmedov, S., Evers, M., 2016. *Bashtepa 2016: preliminary report of the first season of excavations (with an appendix by Aleksandr Naymark)*. Archäologische Mitteilungen aus Iran und Turan 48, 219–264.
- Stark, S., Kidd, F.J., Mirzaakhmedov, J.K., Wang, S., Spengler III, R.N., Mirzaakhmedov, S.J., Silvia, Z., Pozzi, S., Rakhmonov, H., Sligar, M., 2022. The Uzbek-American expedition in Bukhara. Preliminary report on the third season (2017). *Iran* 60, 149–199.
- Swan, C.M., Rehren, T., Lankton, J., Gratuze, B., Brill, R.H., 2017. Compositional observations for Islamic glass from Siraf, Iran, in the Corning Museum of Glass collection. *J. Archaeol. Sci. Rep.* 16, 102–116.
- Weill, D.F., Drake, M.J., 1973. Europium anomaly in plagioclase feldspar: experimental results and semiquantitative model. *Science* 180, 1059–1060.
- Yadav, A.K., Singh, P., 2015. A review of the structures of oxide glasses by Raman spectroscopy. *RSC Adv.* 5, 67583–67609.